

# Hard biaxial ellipsoids revisited: numerical results

Carl M. Bbridge and Enrique Lomba

Instituto de Química Física Rocasolano (CSIC), Serrano 119, 28006 Madrid, Spain

(Dated: November 14, 2006)

Monte Carlo simulations are performed for hard ellipsoids for a number of values of its semi-axes in the range  $c=a=2$  to  $10g$ . The isotropic phase results are compared to the Vesta equation of state [Mol. Phys. 92 651 (1997)]. The position of the isotropic-nematic transition is also evaluated. The biaxial phase is seen to form only after the previous formation of a discotic phase.

## INTRODUCTION

One of the first ever models used in computer simulation studies of the liquid phase was the hard sphere. The next most obvious choice of model is the hard ellipsoid; an affine transformation of the hard sphere. The orientation of the model now becomes a variable within the simulation. Having a model that incorporates orientation facilitates the study of orientationally ordered phases, such as those associated with liquid crystals.

As with hard spheres [1, 2, 3, 4] the first simulations of hard ellipsoids were performed for two-dimensional systems [5, 6]. Hard spheres are only capable of forming two phases; the liquid and the solid. There is no gas-liquid transition, due to the lack of attractive forces. However, the hard ellipsoid system also has a plastic crystal (for small axis ratios) and a nematic phase. Prolate and prolate-like biaxial models, i.e. models of the form  $a > b < c$  with  $b < \sqrt{ac}$  where  $a, b$  and  $c$  are the semi-axes of the ellipsoid, are able to form a uniaxial nematic phase, often denominated as  $N_+$ . Oblate and oblate-like biaxial models, with  $a < b < c$  and  $b > \sqrt{ac}$ , can form a uniaxial 'discotic' phase ( $N_D$ ). A tentative phase diagram for uniaxial ellipsoids was proposed by Frenkel and co-workers [7, 8, 9, 10]. As well as these nematic and discotic phases, Freiser [11] predicted that long-chain molecules could form a biaxial phase  $N_B$ , which has recently been discovered experimentally [12, 13].

The study of hard bodies provide reference systems for use in perturbation theories which add long range attractive interactions [14]. They can also form the monomer units of larger molecules [15, 16]. Hard ellipsoids continue to be of interest [17, 18], having recently been shown that a maximally random jammed (MRJ) packing fraction of  $\phi = 0.7707$  is possible for models whose maximal aspect ratio is greater than  $3$ . [19, 20]. Such high packing fractions were obtained using an 'event-driven' molecular dynamics code [21, 22] and were confirmed experimentally using latex particles and the like [23, 24].

Biaxial ellipsoids have, however, received comparatively little attention, simulations having been performed principally by Allen [25] and by Camp and Allen [26]. Extensive simulation results have been presented previously for uniaxial hard ellipsoids, notably those of Frenkel and Mulder for  $c=a$  in the range  $[1=3;3]$  [9]. In this publication

a number of simulations are performed for biaxial ellipsoids within the region  $c=a$  for  $[0.1;10]$ . Also in this work the isotropic equation of state is compared to theory.

## SIMULATION TECHNIQUE

Standard Metropolis Monte Carlo sampling was used [1]. The decision to reject or accept a trial move for hard bodies is based simply on whether two bodies overlap or not. For hard spheres ( $a = b = c$ ) this criteria is trivial; if the distance between two bodies is less than twice the radius then they overlap. For hard ellipsoids the situation is more complicated, having to take into account the orientations of the ellipsoids as well as the distance between them. One of the first overlap criteria was proposed for two-dimensional ellipsoids by Vieillard-Baron [5, 27]. Perram and Wertheim produced an overlap algorithm for three-dimensional ellipsoids [28]. In this study the Perram-Wertheim criteria was used.

All of the Monte Carlo simulations were performed in the NpT ensemble (with  $k_B T = 1$ ), having cubic boundary conditions, with the system comprising of  $N = 343$  hard ellipsoids. The runs consisted of between 75 and 150 kilocycles for equilibration followed by a further 75–150 kilocycles for the production of thermodynamic data. Each simulation was initiated from the falcon guration of the previous, lower pressure, run. Throughout the simulations the uniaxial order parameter  $S_2$  was monitored for each of the three axis by calculating

$$S_2 = \frac{1}{2} (3 \cos^2 \vartheta_i - 1) ; \quad (1)$$

where  $\vartheta_i$  is the angle between ellipsoid  $i$  and the director vector [29, 30, 31].

The prolate parameters are typified by  $a = b$ , the oblate parameters by  $b = c$  and the biaxial parameters by  $a \neq b \neq c$  where in this work  $a < b < c$  (in this work we define  $a = 1$ ).

Boublik and Nezbeda have shown [32] that hard convex bodies can be described using three geometric expressions; the volume,  $V$ , the surface area,  $S$  and the mean radius of curvature,  $R$ . The second virial coefficient,  $B_2$  for any hard convex body is given by the Isha-Haderiger formula [33, 34], and provides a measure of the excluded

volum e of a molecule' due to the presence of a second molecule,

$$B_2 = R S + V; \quad (2)$$

or

$$\frac{B_2}{V} = 1 + 3; \quad (3)$$

if one de nes the 'non-sphericity' parameter [35]

$$= \frac{R S}{3V}; \quad (4)$$

Values for R , S and V for ellipsoids are provided in Appendix A .

## RESULTS

### Isotropic phase equation of state

Accurate equations of state (EOS) are necessary if the hard ellipsoid uid is to be used as a reference system in perturbation theories. A number of equations of state have been proposed over the years to reproduce the behaviour of the isotropic phase of the ellipsoid system ; notably those of Nezbeda [36], Parsons [37], and Song and Mason [38]. It should be noted that all of these equations of state implicitly assume that the EOS is symmetric with respect to prolate/oblate models, since they are built either directly using  $B_2$ , or indirectly using . This is because  $B_2(1 - 1 - x) = B_2(1 - x - x)$ .

In order to reproduce simulation results, higher virial coefficients are required, where it has been shown that the prolate/oblate symmetry breaks down starting from  $B_3$  [39, 40], as used in the uniaxial EOS of Mason and Solana [41] or the biaxial EOS of Vega [42]. In this work the simulation results are compared to the biaxial Vega equation of state. The Vega EOS is given by

$$Z = 1 + B_2 y + B_3 y^2 + B_4 y^3 + B_5 y^4 + \frac{B_2}{4} \frac{1+y+y^2-y^3}{(1-y)^3} - 1 - 4y - 10y^2 - 18.3648y^3 - 28.2245y^4; \quad (5)$$

where Z is the compressibility factor and y is the volume fraction, given by  $y = V$  where  $V$  is the number density. The virial coefficients are given by the ts

$$B_3 = 10 + 13.094756^0 - 2.073909^0 + 4.096689^{\alpha} + 2.325342^{\alpha} - 5.791266^0; \quad (6)$$

$$B_4 = 18.3648 + 27.714434^0 - 10.2046^0 + 11.142963^{\alpha} + 8.634491^{\alpha} - 28.279451^0 + 17.190946^{\alpha} + 24.188979^0 + 0.74674^{\alpha} - 9.455150^0; \quad (7)$$

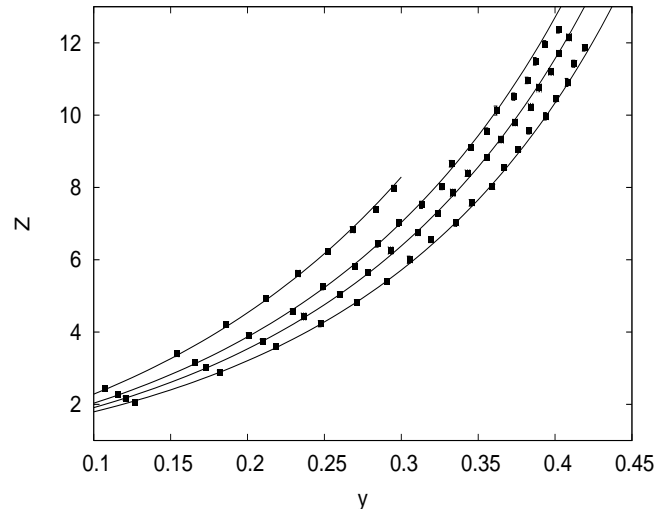


FIG .1: P lot of the simulation results for the biaxialm olecules 1 2 4, 1 2 5, 1 2 6 and the isotropic state points for 1 2 8. The lines are the Vega equation of state.

and

$$B_5 = 28.2245 + 21.288105^0 + 4.525788^0 + 36.032793^{\alpha} + 59.0098^{\alpha} - 118.407497^0 + 24.164622^{\alpha} + 139.766174^0 + 50.490244^{\alpha} - 120.995139^{\alpha} + 12.624655^{\alpha}; \quad (8)$$

where

$$= \frac{4 R^2}{S} - 1; \quad (9)$$

and

$$= \frac{R S}{3V} - 1; \quad (10)$$

Values for R and S for the m odels studied in the work are given in Appendix A .

The effect of varying c for a biaxialm odel is shown in Fig. 1, where various m odels from Table I are plotted. As can be seen, the Vega EOS provides an excellent t for all of the isotropic state points. This is also demonstrated in a plot of the selfdualm odels, where  $b = \frac{P}{\rho ac}$  (Fig. 2) taken from Table II. In gures3 and 4 the isotropic equations of state are plotted for the 1 2:5 2:5, 1 1 2:5 and for the 1 4 4, and 1 1 4 m odels. It can be seen that for these m odels anisotropies the oblate/prolate curves are indeed alm ost coincident, as assumed in the simple EOS built using  $B_2$  only. The num erical results are presented in Tables III and IV .

### Isotropic-liquid crystal transition

The theory behind the isotropic-nematic (I-N ) transition was rst developed by Lars Onsager [43] and was

TABLE I: Equations of state for biaxial ( $a = 1, a < b < c$ ) hard ellipsoids. Error in  $y$  is  $O(10^{-3})$ , error in  $z$  is  $O(10^{-2})$ 

	b = 2; c = 5		b = 2; c = 6		b = 2; c = 8		b = 3; c = 6		b = 3; c = 8		b = 3; c = 10		b = 5; c = 8		b = 5; c = 10		b = 8; c = 10	
P	y	z	y	z	y	z	y	z	y	z	y	z	y	z	y	z	y	z
0.5	0.120	2.17	0.115	2.26	0.107	2.43	0.114	2.28	0.107	2.44	0.102	2.56	0.103	2.52	0.097	2.67	0.093	2.80
1.0	0.173	3.02	0.166	3.15	0.154	3.39	0.165	3.16	0.153	3.40	0.145	3.60	0.146	3.56	0.141	3.70	0.134	3.89
1.5	0.209	3.74	0.200	3.91	0.186	4.21	0.198	3.96	0.196	4.21	0.176	4.45	0.180	4.34	0.170	4.59	0.165	4.74
2.0	0.236	4.42	0.229	4.56	0.211	4.94	0.227	4.60	0.212	4.93	0.200	5.21	0.206	5.06	0.199	5.25	0.194	5.39
2.5	0.259	5.03	0.249	5.25	0.232	5.62	0.246	5.30	0.233	5.60	0.224	5.82	0.226	5.77	0.220	5.93	0.219	5.96
3.0	0.278	5.64	0.270	5.81	0.252	6.22	0.269	5.82	0.253	6.20	0.243	6.45	0.249	6.30	0.243	6.44	0.249	6.29
3.5	0.293	6.25	0.284	6.43	0.268	6.83	0.283	6.45	0.272	6.72	0.258	7.08	0.270	6.76	0.269	6.80	0.286	6.40
4.0	0.310	6.74	0.298	7.01	0.283	7.38	0.297	7.03	0.284	7.36	0.280	7.48	0.288	7.25	0.301	6.95	0.308	6.78
4.5	0.323	7.27	0.313	7.51	0.295	7.97	0.310	7.59	0.302	7.77	0.292	8.05	0.313	7.51	0.320	7.34	0.327	7.19
5.0	0.333	7.85	0.326	8.01	0.310	8.43	0.324	8.06	0.314	8.33	0.310	8.43	0.338	7.73	0.334	7.83	0.341	7.67
5.5	0.343	8.39	0.332	8.65	0.323	8.90	0.333	8.63	0.330	8.70	0.328	8.77	0.352	8.17	0.349	8.23	0.357	8.05
6.0	0.355	8.82	0.345	9.09	0.342	9.16	0.345	9.09	0.338	9.28	0.345	9.08	0.363	8.63	0.361	8.68	0.365	8.58
6.5	0.364	9.32	0.356	9.56	0.357	9.52	0.355	9.58	0.363	9.37	0.355	9.58	0.372	9.13	0.371	9.17	0.377	9.01
7.0	0.374	9.79	0.361	10.12	0.370	9.88	0.362	10.11	0.367	9.98	0.366	9.99	0.388	9.43	0.381	9.60	0.391	9.36
7.5	0.384	10.22	0.373	10.51	0.390	10.05	0.370	10.60	0.379	10.33	0.378	10.37	0.397	9.88	0.391	10.04	0.398	9.84
8.0	0.389	10.75	0.382	10.96	0.395	10.59	0.385	10.87	0.387	10.80	0.389	10.76	0.410	10.20	0.399	10.48	0.409	10.24
8.5	0.397	11.19	0.387	11.48	0.399	11.13	0.394	11.27	0.399	11.13	0.392	11.33	0.414	10.72	0.411	10.81	0.419	10.62
9.0	0.402	11.70	0.393	11.96	0.415	11.35	0.402	11.70	0.406	11.59	0.395	11.90	0.421	11.17	0.415	11.34	0.425	11.06
9.5	0.409	12.15	0.402	12.35	0.421	11.78	0.409	12.15	0.414	12.00	0.408	12.17	0.432	11.49	0.420	11.82	0.432	11.50

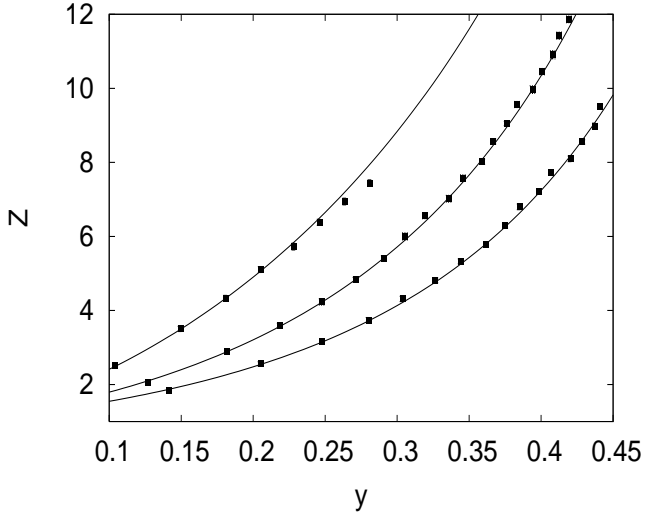


FIG . 2: Plot of the simulation results for the self-dual molecules 1 1:25 1:5625, 1 2 4 and the isotropic state points for 1 3 9. The lines are the Vega equation of state.

TABLE II: Equations of state for biaxial self-dual ( $b = \frac{p}{ac}$ ) hard ellipsoids. Error in  $y$  is  $O(10^{-3})$ , error in  $Z$  is  $O(10^{-2})$   
 $b = 1.25; c = 1.5625$        $b = 2; c = 4$        $b = 3; c = 9$

p	y		y		y	
	b = 1.25; c = 1.5625	b = 2; c = 4	b = 3; c = 9	b = 1.25; c = 1.5625	b = 2; c = 4	b = 3; c = 9
0.5	0.141	1.85	0.126	2.06	0.104	2.51
1.0	0.205	2.55	0.181	2.87	0.149	3.50
1.5	0.247	3.17	0.218	3.59	0.181	4.33
2.0	0.280	3.73	0.247	4.23	0.205	5.10
2.5	0.303	4.31	0.271	4.82	0.228	5.76
3.0	0.326	4.81	0.290	5.40	0.246	6.38
3.5	0.344	5.32	0.305	6.00	0.264	6.94
4.0	0.361	5.79	0.319	6.55	0.281	7.44
4.5	0.375	6.28	0.335	7.01	0.301	7.82
5.0	0.385	6.79	0.345	7.57	0.315	8.29
5.5	0.389	7.22	0.359	8.01	0.332	8.67
6.0	0.406	7.72	0.366	8.56	0.344	9.12
6.5	0.420	8.09	0.376	9.04	0.356	9.54
7.0	0.428	8.55	0.383	9.56	0.364	10.06
7.5	0.437	8.97	0.394	9.96	0.376	10.41
8.0	0.441	9.49	0.400	10.45	0.384	10.88
8.5	0.451	9.86	0.408	10.90	0.395	11.26
9.0	0.458	10.28	0.412	11.42	0.406	11.58
9.5	0.463	10.72	0.419	11.86	0.410	12.11

studied for solutions of hard ellipsoids by Akira Isha [44]. Frenkel and Mulder [9, 10] found an I-N<sub>+</sub> transition for a system of 90–108 prolate ellipsoids of  $c/a = 2.75$ . This result was called into question by Zaragoza et al. [45], suggesting system size effects play an important role in locating the I-N transition. However, a later work by Allen and Mason [46] confirmed the nematic phase for

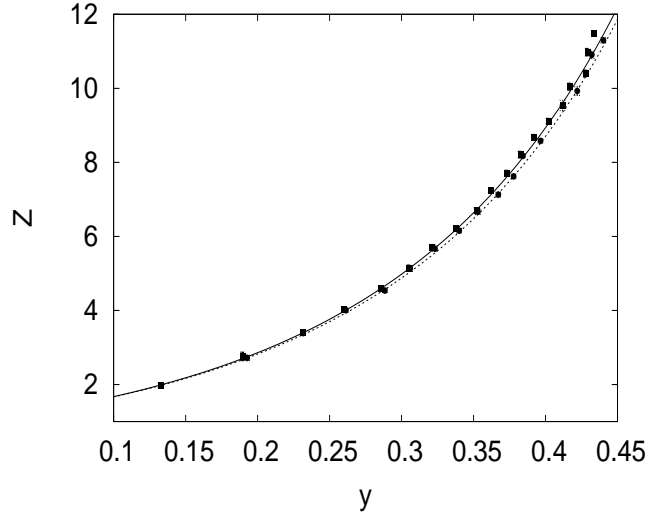


FIG . 3: Plot of the results for the oblate 1 2.5 2.5 model (black squares) and the prolate 1 1 2.5 model (black circles) along with the Vega EOS (oblate: solid line, prolate: dashed line)

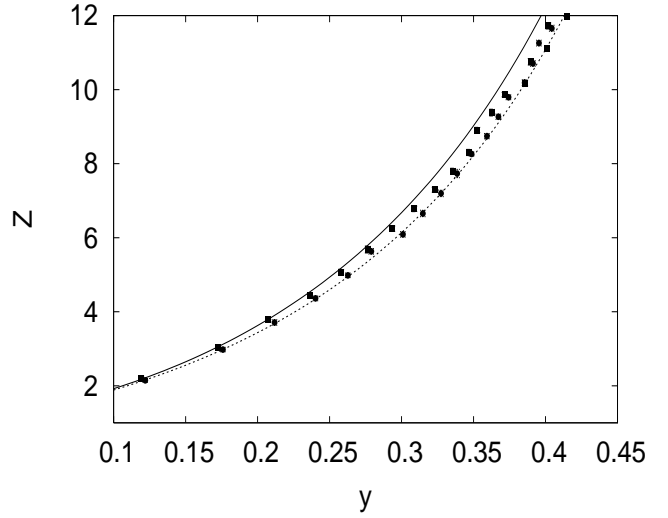


FIG . 4: Plot of the results for the oblate 1 4 4 model (black squares) and the prolate 1 1 4 model (black circles) along with the Vega EOS (oblate: solid line, prolate: dashed line)

$c/a = 3.0$  at densities of  $\rho_{cp} = 0.73$ –0.75. In this work no such transition is found until  $c/a = 6$ . It is interesting to compare this to linear tangent hard spheres, where nematic phases were found for  $m = 6$  and a smectic A phase for  $m = 5$  where  $m$  is the number of monomer units [47]. Note that smectic phases are not observed for hard ellipsoids.

The appearance of the nematic phase for the 1 1 8 (FIG . 7) model was considerably ‘delayed’, and no nematic phase formed for compression runs (150k equilibration followed by 150k production) of the prolate 1 1 10

TABLE III: Equations of state for oblate ( $a = 1, b = c$ ) hard ellipsoids. Error in  $y$  is  $O(10^{-3})$ , error in  $Z$  is  $O(10^{-2})$ 

c	2.5	4	5	6	8	10				
p	y	z	y	z	y	z	y	z	y	z
0.5	0.132	1.97	0.119	2.19	0.113	2.31	0.108	2.41	0.097	2.70
1.0	0.189	2.76	0.172	3.03	0.162	3.23	0.153	3.40	0.140	3.71
1.5	0.231	3.39	0.207	3.78	0.196	4.00	0.185	4.24	0.171	4.57
2.0	0.260	4.02	0.236	4.43	0.220	4.75	0.213	4.91	0.195	5.34
2.5	0.285	4.58	0.258	5.07	0.243	5.38	0.233	5.61	0.226	5.76
3.0	0.305	5.14	0.276	5.68	0.263	5.96	0.252	6.21	0.257	6.10
3.5	0.321	5.70	0.293	6.24	0.282	6.49	0.273	6.69	0.281	6.51
4.0	0.337	6.20	0.308	6.77	0.293	7.13	0.292	7.15	0.307	6.82
4.5	0.352	6.69	0.323	7.29	0.312	7.52	0.306	7.69	0.324	7.26
5.0	0.362	7.23	0.335	7.79	0.325	8.05	0.327	8.00	0.341	7.65
5.5	0.373	7.71	0.346	8.30	0.335	8.58	0.336	8.56	0.351	8.19
6.0	0.382	8.21	0.352	8.90	0.348	9.01	0.355	8.82	0.369	8.50
6.5	0.391	8.68	0.362	9.38	0.358	9.49	0.375	9.07	0.374	9.09
7.0	0.402	9.11	0.371	9.86	0.374	9.78	0.383	9.54	0.394	9.27
7.5	0.412	9.52	0.385	10.17	0.386	10.16	0.394	9.95	0.404	9.70
8.0	0.417	10.04	0.389	10.75	0.398	10.49	0.404	10.34	0.413	10.13
8.5	0.427	10.40	0.400	11.09	0.415	10.72	0.415	10.70	0.416	10.68
9.0	0.429	10.97	0.402	11.72	0.422	11.14	0.424	11.09	0.423	11.12
9.5	0.433	11.47	0.415	11.98	0.437	11.36	0.431	11.53	0.428	11.60

TABLE IV : Equations of state for prolate ( $a = b = 1$ ) hard ellipsoids. Error in  $y$  is  $O(10^{-3})$ , error in  $Z$  is  $O(10^{-2})$ 

c	2.5	4	5	6	8	10		
p	y	z	y	z	y	z	y	z
0.5	0.132	1.97	0.121	2.14	0.115	2.26	0.110	2.37
1.0	0.192	2.71	0.175	2.97	0.166	3.14	0.158	3.29
1.5	0.231	3.38	0.211	3.70	0.200	3.92	0.191	4.09
2.0	0.261	4.00	0.240	4.36	0.226	4.61	0.218	4.80
2.5	0.288	4.53	0.262	4.98	0.250	5.22	0.238	5.48
3.0	0.305	5.13	0.278	5.63	0.268	5.86	0.256	6.13
3.5	0.323	5.67	0.300	6.09	0.282	6.48	0.277	6.59
4.0	0.340	6.15	0.314	6.65	0.300	6.96	0.289	7.23
4.5	0.353	6.66	0.327	7.19	0.314	7.49	0.304	7.74
5.0	0.367	7.12	0.338	7.73	0.325	8.03	0.311	8.40
5.5	0.377	7.62	0.348	8.26	0.332	8.67	0.326	8.82
6.0	0.384	8.17	0.359	8.74	0.346	9.06	0.334	9.39
6.5	0.396	8.58	0.367	9.26	0.352	9.66	0.349	9.72
7.0	0.402	9.10	0.374	9.79	0.365	10.03	0.356	10.27
7.5	0.411	9.53	0.385	10.18	0.373	10.50	0.377	10.40
8.0	0.422	9.92	0.391	10.70	0.375	11.16	0.389	10.76
8.5	0.428	10.39	0.395	11.25	0.388	11.46	0.402	11.06
9.0	0.432	10.90	0.404	11.65	0.394	11.94	0.407	11.55
9.5	0.440	11.29	0.413	12.01	0.403	12.32	0.417	11.90

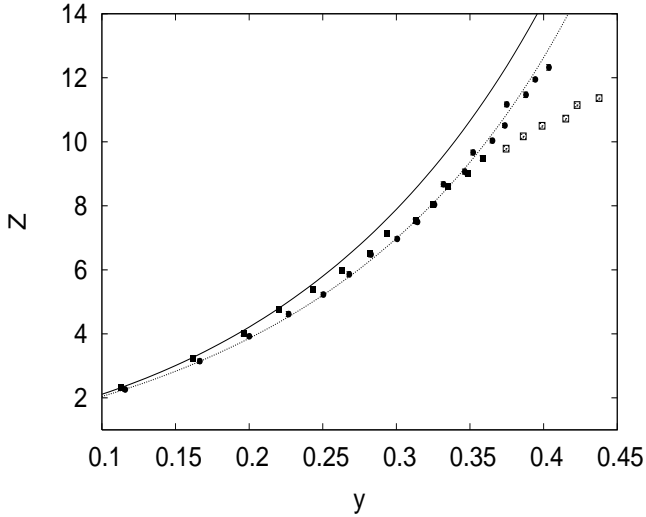


FIG . 5: Plot of the results for the oblate 1 5 5 model (isotropic: black squares, discotic: open squares) and the prolate 1 1 5 model (black circles) along with the Vega EOS (oblate: solid line, prolate: dashed line)

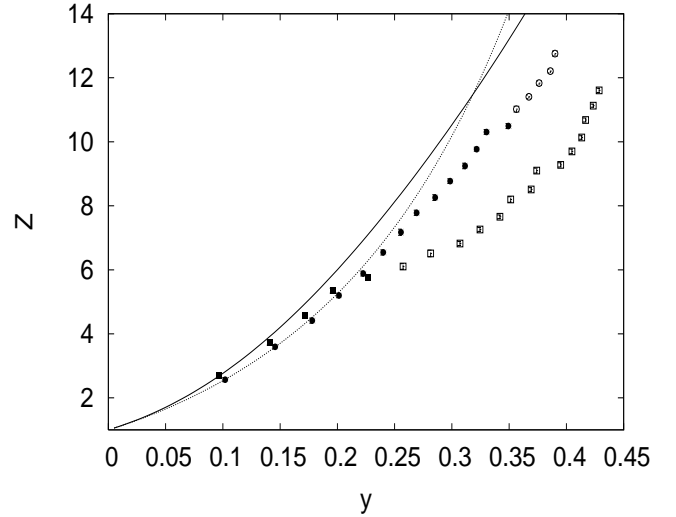


FIG . 7: Plot of isotropic the results for the oblate 1 8 8 model (isotropic: black squares, discotic: open squares) and the prolate 1 1 8 model (black circles, nematic: open circles) along with the Vega EOS (oblate: solid line, prolate: dashed line)

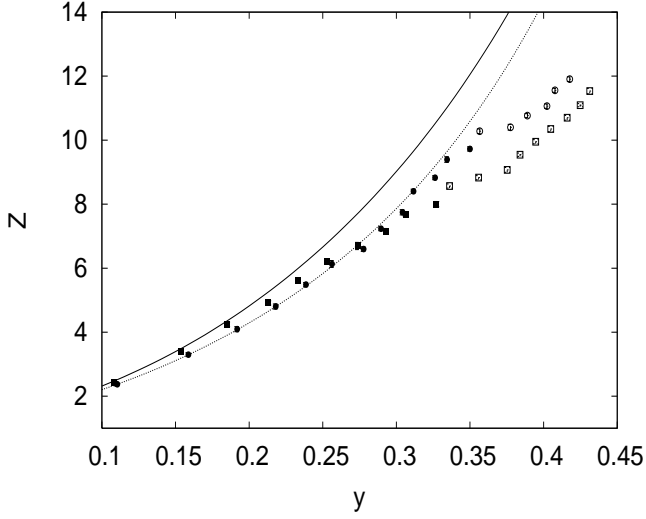


FIG . 6: Plot of isotropic the results for the oblate 1 6 6 model (isotropic: black squares, discotic: open squares) and the prolate 1 1 6 model (isotropic: black circles, nematic: open circles) along with the Vega EOS (oblate: solid line, prolate: dashed line)

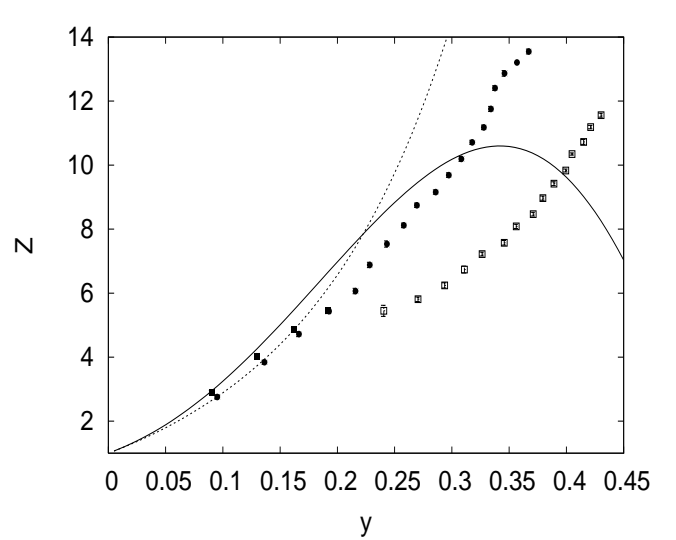


FIG . 8: Plot of the isotropic results for the oblate 1 10 10 model (isotropic: black squares, discotic: open squares) and the prolate 1 1 10 model (black circles) along with the Vega EOS (oblate: solid line, prolate: dashed line)

model (Fig. 8). Given that it is fully expected to see  $N_+$  phases for this model this indicates that so called ‘jamming’ is a real problem for especially elongated prolate systems. The system finds itself grid-locked, and is unable to reorientate into the energetically more favourable nematic phase within the time scale of the simulation. The equation of state of the glassy state (Fig. 8) can be seen to be intermediate between the higher compressibility factor of the isotropic phase, indicated by the Vega

EoS, and the much lower values for the discotic branch of the 1 10 10 model. On the other hand, discotic phases readily appeared for the 1 5 5 model (Fig. 5) upwards.

Samborski et al [48] placed the I-N transition at  $0.370 < y < 0.388$  for the 1 1 5 model,  $0.333 < y < 0.351$  for the 1 5 5 model,  $0.203 < y < 0.222$  for the 1 1 10 model and  $0.185 < y < 0.203$  for the 1 10 10 model. It is interesting to note that I-N transi-

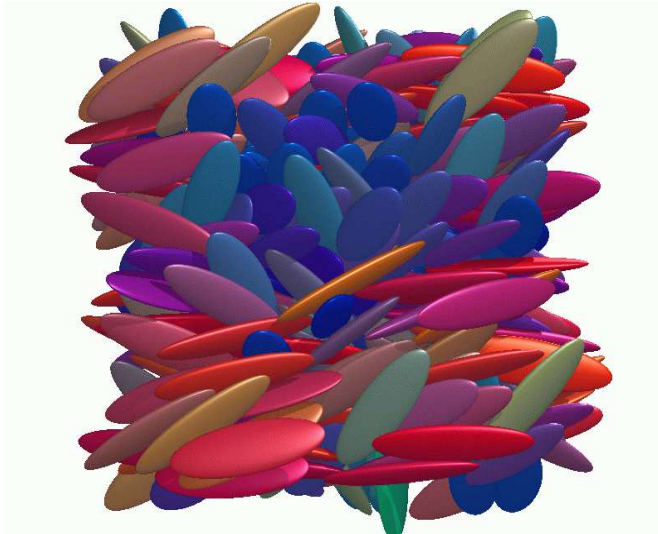


FIG. 9: Snap-shot of the 1 3 10 model in the biaxial phase (here at  $\rho = 8.0$ ). The ellipsoids are colour coded with respect to their orientations (colour online).

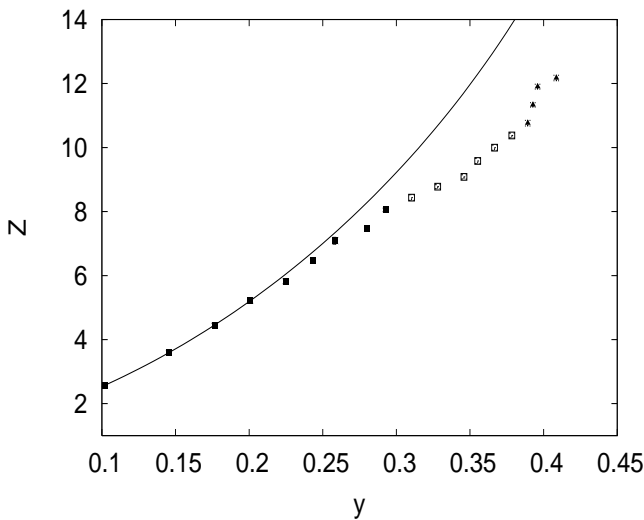


FIG. 10: Plot of the equation of state for the biaxial 1 3 10 model (isotropic: black squares, discotic: open squares, biaxial: black triangles) along with the Vega EOS for the isotropic branch.

tion sets in at lower volume fractions for oblate ellipsoids than for prolate models that have the same value of  $c$ . The same is seen in this work for the 8' (Fig. 6) and 8'' (Fig. 7) models. This is probably due to the fact that the compressibility factor of the oblate models, for a given volume fraction, is higher than that of its corresponding prolate counterpart. This triggers the earlier onset of the I-N transition.

In this study only one convincing biaxial phase was identified, that of the 1 3 10 model (see Fig. 9 for a snapshot, Fig. 10 for the EOS). The biaxial phase

formed at  $\rho = 8.0$ , however, at  $\rho = 5.0$  the system had formed a discotic phase. This indicates that the formation of a biaxial phase is a two-stage process; first orientating along the short  $a$  axis, later followed by the long  $c$  axis i.e. having the phase transitions isotropic - discotic - biaxial. This is in line with the observation that discotic phases form at lower volume fractions than nematic phases (the biaxial phase can be seen as being composed of both a discotic and a nematic phase).

The positions of the isotropic liquid-liquid crystal transitions found in this work are presented in Table V. A study of the I-N transition for biaxial ellipsoids was undertaken by Tjepko-Margo and Evans [49] confirming the finding of Gelfbart and Barboy [50] that biaxiality reduces the first order nature of the I-N transition (this result was also confirmed for hard spheroplatelets by Somozza and Tarazona [51]). It appears that the additional degree of freedom associated with biaxiality increases the disorder in the nematic phase with respect to a uniaxial ( $D_{1h}$ ) model. At the 'self-dual' point (where  $a:b = b:c$ , i.e.  $b = \sqrt{ac}$ ) the transition becomes second-order [52]. The isotropic-biaxial nematic transition is said to occur for models that are close to this self-dual point [25]. For the uniaxial 1 10 10 models a considerable jump can be seen in the volume fractions associated with the formation of the discotic phase (Fig. 8), one of the hallmarks of a first-order transition. Meanwhile, for the biaxial 1 3 10 model no such jump is seen.

## CONCLUSIONS

Various ellipsoidal models have been subjected to Monte Carlo compression runs. The Vega equation of state is seen to perform very well for the isotropic phases of all of the models considered. The elongated uniaxial models show indications of the first-order nature of the isotropic-nematic transition. However, the formation of orientationally ordered phases for very long prolate models is severely hindered by the formation of a glass-like state. The oblate models form discotic readily, at lower volume fractions than their prolate partners. The biaxial phase seems to form in a two-stage process, first forming a discotic phase, followed by the biaxial phase upon orientation of the long axes.

The authors should like to thank C. Vega for the provision of the Perram-Wertheim overlap algorithm and N.G. Almarza for useful discussions. This work was funded by project FIS2004-02954-C03-02 of the Spanish Ministerio de Educacion y Ciencia, and by project S-0505/ESP/0299 - CSIC QFT (MOSSNOHO) of the D.G. de Universidades e Investigación del Comunidad de Madrid. One of the authors (C.M.) would like to thank the CSIC for the award of an I3P post-doctoral contract.

TABLE V : Location of the isotropic-nematic transition ( $S_2 > 0.4$ ) for hard ellipsoids (Note:  $a = 1$ ). Order parameters are given for  $p = 9.5$ .

b	c	p	y	phase	$S_2(c)$	$S_2(a)$
<b>prolate</b>						
1	2.5	{	{	I	< 0.1	< 0.1
1	4	{	{	I	< 0.1	< 0.1
1	5	{	{	I	0.13	< 0.1
1	6	7.0	0.356	N <sub>+</sub>	0.69	0.20
1	8	7.5	0.356	N <sub>+</sub>	0.55	0.18
1	10	{	{	I	0.30	0.12
<b>oblate</b>						
2.5	2.5	{	{	I	< 0.1	< 0.1
4	4	{	{	I	0.12	0.24
5	5	7.0	0.374	N	0.23	0.81
6	6	5.5	0.336	N	0.25	0.87
8	8	3.0	0.257	N	0.26	0.92
10	10	2.5	0.240	N	0.27	0.95
<b>biaxial prolate</b> ( $b < \frac{p}{ac}$ )						
2	5	{	{	I	0.10	< 0.1
2	6	{	{	I	0.21	0.15
2	8	6.0	0.342	N <sub>+</sub>	0.85	0.25
3	10	8.0	0.389	B	0.48	0.76
<b>biaxial self-dual</b>						
1.25	1.5625	{	{	I	< 0.1	< 0.1
2	4	{	{	I	< 0.1	< 0.1
3	9	4.5	0.30	N	0.34	0.81
<b>biaxial oblate</b> ( $b > \frac{p}{ac}$ )						
3	6	9.0	0.402	N	0.23	0.46
3	8	6.0	0.338	N	0.27	0.78
5	8	4.5	0.313	N	0.25	0.90
5	10	3.5	0.269	N	0.30	0.92
8	10	3.0	0.249	N	0.27	0.95

#### APPENDIX A

In Table V I we provide a table of  $R$ ,  $S$ ,  $V$ , and  $B_2=V$  for the various models studied in this work. The values for  $R$  and  $S$  are obtained by evaluating the expressions derived by Singh and Kumar [53, 54]. Thus the mean radius of curvature is given by

$$R = \frac{a}{2} \frac{r}{\sqrt{1 + \frac{b}{c}}} + \frac{p}{c} \frac{1}{c} F(\theta; k_1) + E(\theta; k_1); \quad (11)$$

and the surface area by

$$S = 2 \pi^2 a^2 \left( 1 + \frac{p}{c} \frac{1}{\sqrt{1 + \frac{b}{c}}} \right) \frac{1}{c} F(\theta; k_2) + E(\theta; k_2); \quad (12)$$

where  $F(\theta; k)$  is an elliptic integral of the first kind and  $E(\theta; k)$  is an elliptic integral of the second kind, with the

TABLE VI: Values for  $R$ ,  $S$ ,  $V$ , and  $B_2=V$  for hard ellipsoids (Note:  $a = 1$ ).

b	c	R	S	V		$B_2=V$
<b>sphere</b>						
1	1	1	4	4 =3	1	4
<b>prolate</b>						
1	2.5	1.5919	26.1518	10.472	1.32516	4.97549
1	4	2.26639	40.4975	16 =3	1.82597	6.4779
1	5	2.73397	50.1925	20 =3	2.184	7.552
1	6	3.20942	59.9386	8	2.55136	8.65409
1	8	4.17441	79.5147	32 =3	3.30174	10.9052
1	10	5.15042	99.151	40 =3	4.06377	13.1913
<b>oblate</b>						
2.5	2.5	2.0811	50.0111	26.1799	1.32516	4.97549
4	4	3.22269	113.921	64 =3	1.82597	6.4779
5	5	3.99419	171.78	100 =3	2.184	7.552
6	6	4.76976	241.985	48	2.55136	8.65409
8	8	6.32758	419.657	256 =3	3.30174	10.9052
10	10	7.89019	647.22	400 =3	4.06377	13.1913
<b>biaxial</b>						
1.25	1.5625	1.28328	20.1576	8.18123	1.05395	4.16185
2	4	2.52566	63.4766	32 =3	1.59473	5.7842
2	5	2.96925	78.2743	40 =3	1.84951	6.54853
2	6	3.42527	93.1895	16	2.11675	7.35026
2	8	4.36059	123.218	64 =3	2.67234	9.01701
3	6	3.70789	129.13	24	2.11675	7.35026
3	8	4.60996	170.448	32	2.60536	8.81607
3	9	5.07182	191.203	36	2.85815	9.57446
3	10	5.53883	212.0	40	3.11474	10.3442
5	8	5.22725	268.73	160 =3	2.7946	9.38379
5	10	6.10332	333.946	200 =3	3.24386	10.7316
8	10	7.1304	521.211	320 =3	3.69682	12.0904

amplitude being

$$\theta' = \tan^{-1} \left( \frac{p}{c} \right); \quad (13)$$

and the moduli

$$k_1 = \sqrt{\frac{c}{c - b}}; \quad (14)$$

and

$$k_2 = \sqrt{\frac{b(1 + \frac{b}{c})}{c(1 + \frac{b}{c})}}; \quad (15)$$

where the anisotropy parameters,  $b$  and  $c$ , are

$$b = \frac{b^2}{a} - 1; \quad (16)$$

and

$$c = \frac{c^2}{a} - 1; \quad (17)$$

The volume of the ellipsoid is given by the well known

$$V = \frac{4}{3}abc \quad (18)$$

Note the symmetry between the prolate and oblate ellipsoids for the values of  $\epsilon$ , and thus for  $B_2$ .

---

- [1] N. Metropolis, A. W. Rosenbluth, M. N. Rosenbluth, A. H. Teller, and E. Teller, *J. Chem. Phys.* 21, 1087 (1953).
- [2] B. J. Alder and T. E. Wainwright, *J. Chem. Phys.* 27, 1208 (1957).
- [3] W. W. Wood, Los Alamos Scientific Laboratory Report LA-2827 (1963).
- [4] W. W. Wood, *J. Chem. Phys.* 52, 729 (1970).
- [5] J. V. Jeillard-Baron, *J. Chem. Phys.* 56, 4729 (1972).
- [6] J. A. Cuesta and D. Frenkel, *Phys. Rev. A* 42, 2126 (1990).
- [7] D. Frenkel, B. M. Mulder, and J. P. McTague, *Phys. Rev. Lett.* 52, 287 (1984).
- [8] B. Evans, *Molec. Phys.* 100, 199 (2002).
- [9] D. Frenkel and B. M. Mulder, *Molec. Phys.* 55, 1171 (1985).
- [10] B. Mulder and D. Frenkel, *Molec. Phys.* 55, 1193 (1985).
- [11] M. J. Freiser, *Phys. Rev. Lett.* 24, 1041 (1970).
- [12] L. A. Madsen, T. J. Dingemans, M. Nakata, and E. T. Samulski, *Phys. Rev. Lett.* 92, 145505 (2004).
- [13] B. R. Acharya, A. Prakash, and S. Kumar, *Phys. Rev. Lett.* 92, 145506 (2004).
- [14] J. W. Perram and E. Praestgaard, *Molec. Phys.* 63, 1103 (1988).
- [15] C. McBride and C. Vega, *J. Chem. Phys.* 117, 10370 (2002).
- [16] G.-W. Wu and R. J. Sadus, *Fluid Phase Equilib.* 194, 227 (2002).
- [17] M. Murat and Y. Kantor, *Phys. Rev. E* 74, 031124 (2006).
- [18] C. D. Michele, A. Scala, R. Schilling, and F. Sciortino, *J. Chem. Phys.* 124, 104509 (2006).
- [19] A. Donev, I. Cisse, D. Sachs, E. A. Variano, F. H. Stillinger, R. Connolly, S. Torquato, and P. M. Chaikin, *Science* 303, 990 (2004).
- [20] A. Donev, F. H. Stillinger, P. M. Chaikin, and S. Torquato, *Phys. Rev. Lett.* 92, 255506 (2004).
- [21] A. Donev, S. Torquato, and F. H. Stillinger, *J. Comput. Phys.* 202, 737 (2005).
- [22] A. Donev, S. Torquato, and F. H. Stillinger, *J. Comput. Phys.* 202, 765 (2005).
- [23] M. G. Basavaraj, G. G. Fuller, J. Fransaer, and J. Verma, *Langmuir* 22, 6605 (2006).
- [24] W. Man, A. Donev, F. H. Stillinger, M. T. Sullivan, W. B. Russel, D. Heeger, S. Inati, S. Torquato, and P. M. Chaikin, *Phys. Rev. Lett.* 94, 198001 (2005).
- [25] M. P. Allen, *Liq. Cryst.* 8, 499 (1990).
- [26] P. J. Camp and M. P. Allen, *J. Chem. Phys.* 106, 6681 (1997).
- [27] W. Wang, J. Wang, and M.-S. Kim, *Computer Aided Geometric Design* 18, 531 (2001).
- [28] J. W. Perram and M. S. Wertheim, *J. Comput. Phys.* 58, 409 (1985).
- [29] J. P. Straley, *Phys. Rev. A* 10, 1881 (1974).
- [30] R. Eppenga and D. Frenkel, *Molec. Phys.* 52, 1303 (1984).
- [31] C. Zannoni, in *The Molecular physics of liquid crystals*, edited by G. R. Luckhurst and G. W. Gray (Academic Press, 1979), chap. 3, p. 51.
- [32] T. Boublík and I. Nezbeda, *Coll. Czech. Chem. Commun.* 51, 2301 (1986).
- [33] A. Ishihara, *J. Chem. Phys.* 18, 1446 (1950).
- [34] A. Ishihara and T. Hayashida, *J. Phys. Soc. Jpn.* 6, 40 (1951).
- [35] A. Ishihara and T. Hayashida, *J. Phys. Soc. Jpn.* 6, 46 (1951).
- [36] I. Nezbeda, *Chem. Phys. Lett.* 41, 55 (1976).
- [37] J. D. Parsons, *Phys. Rev. A* 19, 1225 (1979).
- [38] Y. Song and E. A. Mason, *Phys. Rev. A* 41, 3121 (1990).
- [39] M. Rigby, *Molec. Phys.* 66, 1261 (1989).
- [40] M. S. Wertheim, *Molec. Phys.* 99, 187 (2001).
- [41] M. Maleso and J. Solana, *Molec. Phys.* 79, 1365 (1993).
- [42] C. Vega, *Molec. Phys.* 92, 651 (1997).
- [43] L. Onsager, *Ann. N.Y. Acad. Sci.* 51, 627 (1949).
- [44] A. Ishihara, *J. Chem. Phys.* 19, 1142 (1951).
- [45] G. Zamagnochea, D. Levesque, and J. Weiss, *Molec. Phys.* 75, 989 (1992).
- [46] M. P. Allen and C. P. Mason, *Molec. Phys.* 86, 467 (1995).
- [47] C. Vega, C. McBride, and L. G. MacDowell, *J. Chem. Phys.* 115, 4203 (2001).
- [48] A. Samorski, G. T. Evans, C. P. Mason, and M. Allen, *Molec. Phys.* 81, 263 (1994).
- [49] B. Tjepkemoargo and G. T. Evans, *J. Chem. Phys.* 94, 4546 (1991).
- [50] W. M. Gelbart and B. Barboy, *Accounts of Chemical Research* 13, 290 (1980).
- [51] A. M. Somozas and P. Tarazona, *Molec. Phys.* 75, 17 (1992).
- [52] B. Mulder, *Phys. Rev. A* 39, 360 (1989).
- [53] G. S. Singh and B. Kumar, *J. Chem. Phys.* 105, 2429 (1996).
- [54] G. S. Singh and B. Kumar, *Annals of Physics* 294, 24 (2001).